

sponds to its isoelectric point, a negative charge is formed on the surface which is neutralized by adsorbed cations.

When supported Pt-Ru bimetallic catalysts were prepared from aqueous solutions of $\text{H}_2\text{PtCl}_6 \cdot 6\text{H}_2\text{O}$ and $\text{RuCl}_3 \cdot 3\text{H}_2\text{O}$ (2, 3), it was found that the surface of the resulting bimetallic particles was strongly enriched in Pt. It was suggested that this surface enrichment occurred because the interactions between the Pt precursor and the support were predominantly anionic while the speciation of the Ru precursor was cationic. Because the impregnation was carried out at a pH which was slightly higher than that corresponding to the isoelectric point of silica (IEP), the surface was negatively charged. This negative surface charge results in the preferential attachment of the cationic precursors. These are strongly bound due to the resulting electrical double layer (8).

In a succeeding study, a reversal in the surface composition was obtained when a Pt/SiO₂ catalyst prepared using an aqueous solution of H_2PtCl_6 was sequentially impregnated with a benzene solution of ruthenocene [bis(cyclopentadienyl)ruthenium, $(\text{C}_5\text{H}_5)_2\text{Ru}$] (10). The weak interaction between ruthenocene, dissolved in the organic solvent, and the support, resulted in the rapid surface diffusion of the ruthenium precursor across the support. This interaction is weak and predominantly physical in nature. When the decomposition was carried out in flowing H_2 , the ruthenocene was rapidly reduced when its ligands interacted with hydrogen chemisorbed on reduced Pt sites.

Because of these results it was decided to perform a study in which both the Pt and the Ru precursors interact strongly with the support. For this purpose $\text{Pt}(\text{NH}_3)_4(\text{NO}_3)_2$ and $\text{Ru}(\text{NH}_3)_6\text{Cl}_3$ were selected as metal precursors. Because both of these precursors [$\text{Pt}(\text{NH}_3)_4$]²⁺ and [$\text{Ru}(\text{NH}_3)_6$]³⁺ are cationic, they are strongly bound to the surface of silica which is negatively charged at the pH of 9 used in the coimpregnation. At

a pH higher than 10, substantial dissolution of the silica support occurs (8).

Of particular interest to us in this study was to seek answers to the following questions: (1) Are bimetallic particles formed when catalysts are prepared from strongly interacting metal precursors? (2) What is the surface composition of the resulting bimetallic particles if they are indeed formed? and (3) What is the elemental bulk composition of the bimetallic particles formed and does this composition depend on particle size?

EXPERIMENTAL

Catalyst preparation. Cab-O-Sil (Grade M-5, surface area 200 m²/g, average pore diameter 14 nm), obtained from the Cabot Corp. (Boston MA), was first treated with 0.1 M HNO_3 in order to remove traces of alkali metal ions. It was then washed and suspended in distilled, doubly deionized water. The pH of the resulting suspension (~3) was adjusted to a pH of 9 by the addition of 1 M NH_4OH . An aqueous solution of the metal precursors (obtained from the Strem Chemical Co., Newburyport, MA) sufficient to ensure a total metal loading of 0.3 mmol of metal per gram of support was added. The pH of the resulting solution decreased to about 7-8 following the addition of the metal precursors and was readjusted to 9 through further addition of NH_4OH . The solution was continuously stirred for 12 h followed by filtering and washing with doubly distilled, deionized water. The purpose of washing was to remove weakly adsorbed metal precursors and to eliminate chloride ions which have been shown to interfere with subsequent chemisorption and surface titration measurements (11-13). The resulting mono- and bimetallic catalysts were dried under vacuum in a desiccator at room temperature and analyzed for Pt and Ru metal loading content by induced coupled plasma (Galbraith Laboratories, Knoxville, TN). Reduction of the mono- and bimetallic catalysts prepared by this method was carried out in flowing H_2 at

673 K for 4 h. Due to the unstable nature of $\text{Ru}(\text{NH}_3)_6\text{Cl}_3$ it was found necessary to reduce the catalysts immediately following preparation.

Surface composition and dispersion measurements. The surface composition measurements of the resulting bimetallic catalysts were performed by titrating a monolayer of chemisorbed oxygen with CO to a CO_2 endpoint. The selective O_2 -CO titration was performed by the dynamic pulse method as outlined in previous studies (1-3, 14). Dispersion measurements of the monometallic catalysts were performed using CO chemisorption. The dispersion of the bimetallic catalysts was obtained by measuring the uptake of O_2 during the selective O_2 -CO titration. In all cases, dispersions obtained by chemisorption were cross checked by transmission electron microscopy.

All gases used in this study were Ultra-high Purity Grade (99.99% pure) and were purchased from the Linco Co. of Chicago, Illinois. They were further purified by passing them through dry ice/acetone traps which were kept at a temperature of 195 K. Two Supelco high capacity gas purifiers were used to further purify the hydrogen and helium streams. In the case of helium, which was the carrier gas, a final purification was performed through the use of a Supelco OMI-1 indicator trap.

Electron microscopy studies. Particle size determinations were carried out using a modified JEOL 100CX microscope equipped with a STEM attachment. Approximately 1000 particles were randomly analyzed on the TEM micrographs. To ensure that these particles were representative, three different TEM specimens, each containing a different batch of sample, were used to obtain the corresponding micrographs. Samples were prepared by ultrasonically dispersing the catalyst powder in absolute isopropanol. A drop of this suspension was placed on carbon-coated copper grids followed by drying under infrared radiation. The determination of the elemen-

tal composition was performed on a VG HB 501 electron microscope at the University of Wisconsin. This was a dedicated STEM equipped with a field emission gun. Using this instrument it was possible to focus the electron beam to a diameter of 1.5 to 2.0 nm. The quantitative analysis of the EDXS spectra were carried out using a standard-less-thin-film technique. Integrated intensities of the platinum and ruthenium X-ray lines were obtained using a least-square-digital filter routine. Because the specimens were essentially transparent to the electron beam, the Cliff-Lorimer approach was used directly. Corrections for absorption and secondary fluorescence were found to be unnecessary (15). Use of this microscope enabled the analysis of bimetallic particles as small as 1.0 nm.

Diffuse UV reflectance studies. In order to study the possibility that structural changes in the precursor may have occurred as the result of adsorption, diffuse UV reflectance studies were performed on the precursor adsorbed on the support. Spectral features were compared to those obtained for the precursor dissolved in solution.

The diffuse UV spectra were obtained by placing the sample in a specially designed UV cell-reactor. An integrating sphere which was connected to the Perkin-Elmer Lambda-5 spectrophotometer through fiber optic cables was used to record the spectra. Details of the design of the UV cell-reactor and other pertinent instrumentation are found elsewhere (3). The spectral data obtained were processed using a Perkin-Elmer Model 3600 data station.

RESULTS

Diffuse UV reflectance studies. A comparison of the UV spectrum of $[\text{Pt}(\text{NH}_3)_4]^{2+}/\text{SiO}_2$ to that of the precursor in solution is shown in Fig. 1. The structure of $[\text{Pt}(\text{NH}_3)_4]^{2+}$ has been shown to be square planar with two H_2O ligands occupying axial positions to give an overall tetragonal bipyramid configuration (16). An intense

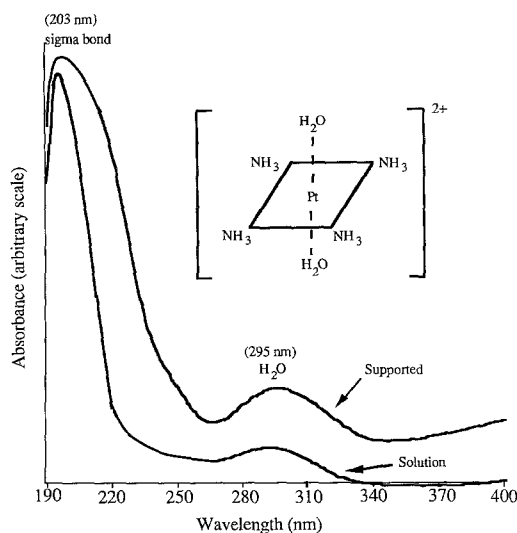


FIG. 1. A comparison of the UV spectrum of $[\text{Pt}(\text{NH}_3)_4]^{2+}$ in aqueous solution to that of $[\text{Pt}(\text{NH}_3)_4]^{2+}$ adsorbed on silica.

charge transfer band due to the σ bonds of the NH_3 ligands was observed at 203 nm. The position of this σ band was identical for both the supported complex and the complex in solution. A weak charge transfer band due to the σ bonds of the two H_2O ligands was observed at 295 nm. This band was present in both spectra and its position was not observed to shift. From these results it was concluded that the structure of the platinum precursor was not significantly altered during the adsorption process.

Similar studies performed on $[\text{Ru}(\text{NH}_3)_6]^{3+}$ are shown in Fig. 2. A single charge transfer band centered at 280 nm was observed for both the freshly prepared supported complex and the complex in solution. This charge transfer band has been assigned to the σ bonding of the NH_3 ligands which are octahedrally coordinated to the centrally located Ru atom. These findings are consistent with those reported by Pearce *et al.* (17). The UV spectrum of $[\text{Ru}(\text{NH}_3)_6]^{3+}$ is air sensitive. Significant changes were observed during aging of the unreduced catalyst. Polymerization of the

complex occurs following exposure to air after approximately 5 h. For this reason, the catalyst must be reduced as soon as possible after drying. The air sensitivity of $[\text{Pt}(\text{NH}_3)_4]^{2+}/\text{SiO}_2$ was somewhat less than that observed for $[\text{Ru}(\text{NH}_3)_6]^{3+}$. However, decomposition occurs following exposure to air for several days.

The UV data of the freshly adsorbed precursors, therefore, suggests that the adsorption of both Pt and the Ru metal precursors involves little or no perturbation of their structure in solution.

Metal dispersion considerations. It was found that catalyst pretreatment of the supported monometallic catalysts was an important variable in the preparation of highly dispersed catalysts. This observation is summarized in Fig. 3. The direct reduction of $[\text{Pt}(\text{NH}_3)_4]^{2+}$ in H_2 for 4 h at 673 K leads to Pt dispersions of about 40%. The average particle size of these catalysts was between 2.5 and 3.0 nm. When $[\text{Pt}(\text{NH}_3)_4]^{2+}/\text{SiO}_2$ was treated with O_2 for 1 h at 573 K prior to reduction in H_2 at 673 K, a Pt dispersion of 80% was obtained. The average particle size as determined by transmission electron microscopy was between 1.0 and 1.5 nm.

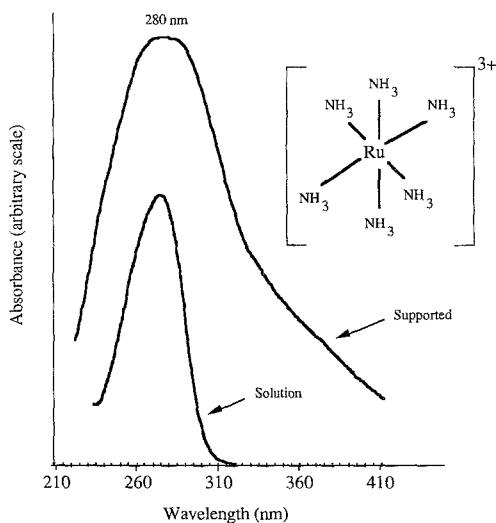


FIG. 2. A comparison of the UV spectrum of $[\text{Ru}(\text{NH}_3)_6]^{3+}$ in aqueous solution to that of $[\text{Ru}(\text{NH}_3)_6]^{3+}$ adsorbed on silica.

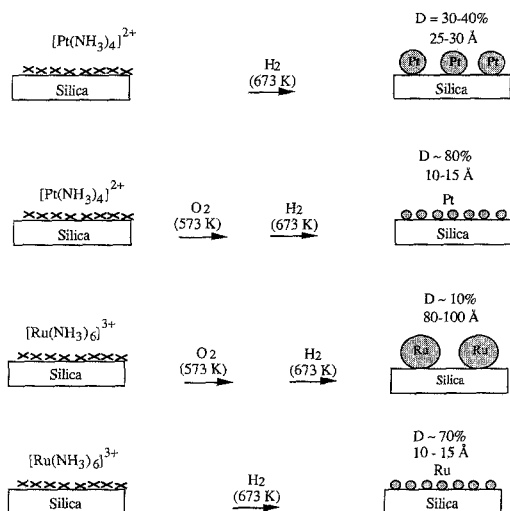


FIG. 3. Effect of pretreatment on the metal dispersion of silica-supported Pt and Ru catalysts.

The $[\text{Ru}(\text{NH}_3)_6]^{3+}/\text{SiO}_2$ metal complex showed a completely different behavior. Pretreatment in O_2 at 573 K followed by reduction in H_2 at 673 K resulted in the formation of poorly dispersed ($\sim 10\%$), large Ru particles. The average Ru particle size was determined to be between 8.0 and 10 nm. When the $[\text{Ru}(\text{NH}_3)_6]^{3+}/\text{SiO}_2$ metal complex was reduced directly in H_2 at 673 K a highly dispersed catalyst (70%) was obtained. The average Ru particle size was calculated to be between 1.0 and 1.5 nm. The effect of oxygen on the dispersion of the Ru/SiO_2 is significant and this striking difference in the metal particle size is readily apparent in the TEM images of these samples. Figure 4 shows representative micrographs of two Ru/SiO_2 samples. One was treated with oxygen prior to reduction (Fig. 4a) and the other was directly reduced in hydrogen (Fig. 4b). Comparison of these two micrographs shows that treatment in oxygen at 573 K prior to reduction leads to an eightfold decrease in the size of the ruthenium particles. The effect of oxygen pretreatment, therefore, appears to be considerably larger in the case of the Ru precursor than that observed for Pt.

Because of these considerations, direct

TABLE 1

Metal Loadings of Pt–Ru/ SiO_2 Catalysts

ID	Pt wt%	Ru wt%	mmoles Pt per g support	mmoles Ru per g support	mmoles metal per g support
IV1	2.68	0.00	0.14	0.00	0.14
IV2	1.16	0.61	0.06	0.06	0.12
IV3	0.98	1.03	0.05	0.10	0.15
IV4	0.19	1.12	0.01	0.11	0.12
IV5	0.00	1.00	0.00	0.10	0.10

reduction in H_2 was used as a compromise to obtain the highest possible dispersion of the supported Pt–Ru/ SiO_2 bimetallic clusters. In addition to the supported monometallic catalysts, three Pt–Ru bimetallic catalysts having different weight loadings were prepared. The final metal loadings and composition of these catalysts as determined by ICP analysis are shown in Table 1. The total metal loading in terms of mmoles metal/gram of support varied only slightly between 0.10 for Ru to 0.14 for Pt. It is interesting to note that when $[\text{Pt}(\text{NH}_3)_4]^{2+}$ and $[\text{Ru}(\text{NH}_3)_6]^{3+}$ were coadsorbed, washing with deionized water lead to the preferential adsorption of $[\text{Ru}(\text{NH}_3)_6]^{3+}$. For example, the catalyst (IV3) prepared by adsorbing 0.15 mmol of Pt and 0.15 mmol of Ru gave a final metal loading after washing of 0.05 mmol of Pt and 0.10 mmol of Ru.

The metal dispersion as determined from the O_2 –CO titration experiments and the particle sizes as measured by TEM for all of the monometallic and bimetallic catalysts prepared are summarized in Table 2. The

TABLE 2

Total Metal Dispersion and Particle Sizes of Monometallic and Bimetallic Catalysts

ID	Pt/(Pt + Ru)	Dispersion (O_2)	Particle Size (TEM) d (Å)
IV1	1.00	39%	25
IV2	0.50	52%	20
IV3	0.33	59%	18
IV4	0.08	61%	14
IV5	0.00	67%	10

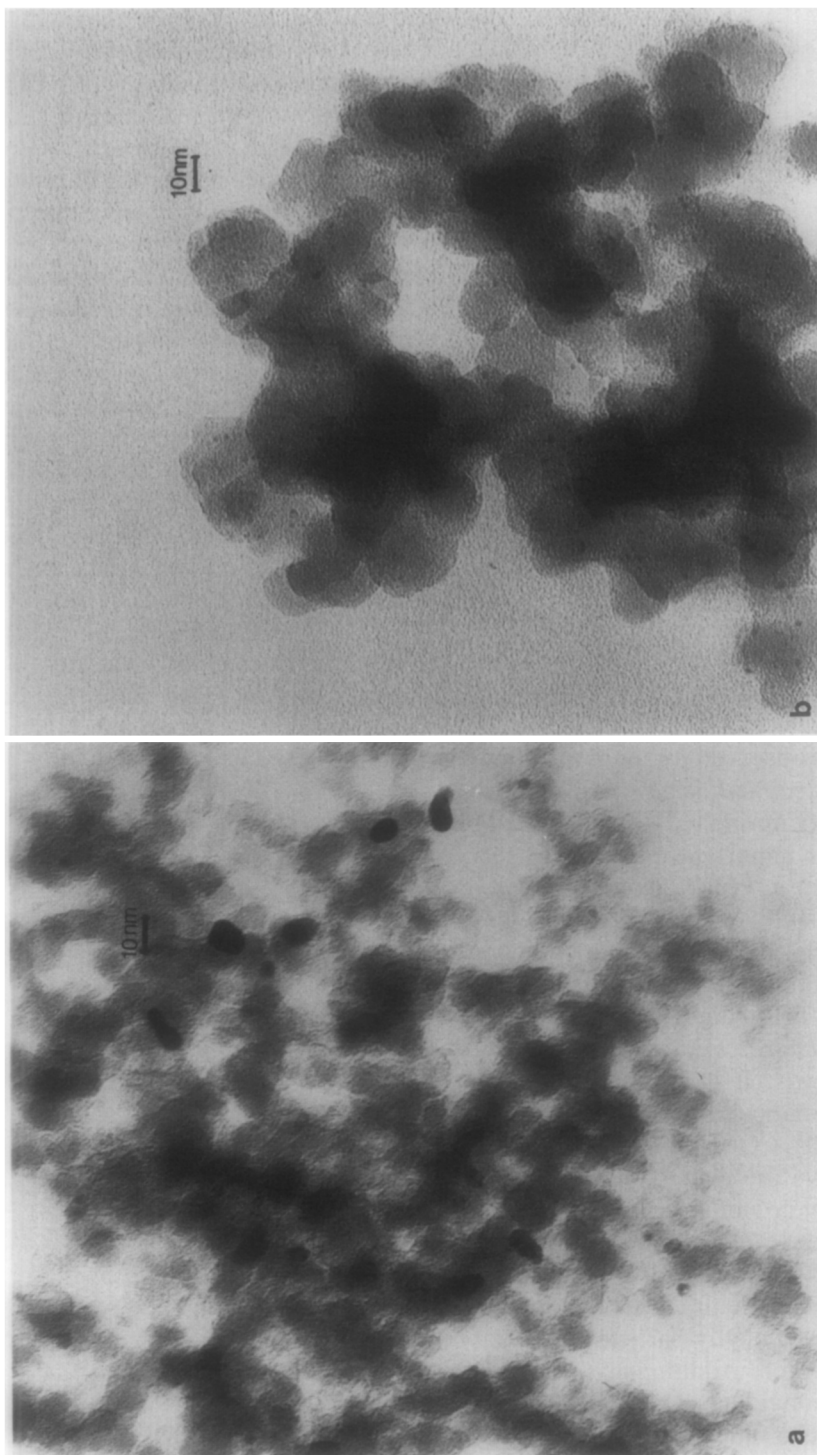


FIG. 4. TEM bright field images of Ru/SiO₂. (a) Sample treated with oxygen at 573 K prior to hydrogen reduction at 673 K. (b) Sample directly reduced in hydrogen at 673 K.

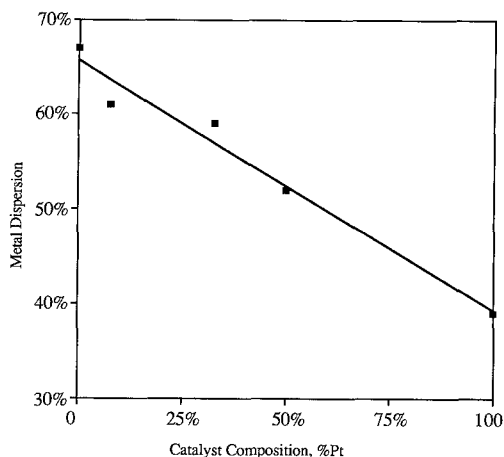


Fig. 5. Metal dispersion as a function of catalyst composition.

metal dispersion decreased linearly with increasing Pt content (Fig. 5).

Surface composition measurements. The surface composition measurements as determined by the selective O_2 -CO titration method are shown in Fig. 6. Surface enrichment in Pt was observed for all of the bimetallic catalysts studied, suggesting a higher surface mobility during reduction for the Pt precursor. It is important to note that surface enrichment in Pt for the catalysts prepared in this study was considerably less than that observed for bimetallic catalysts prepared from the coimpregnation of silica with $H_2PtCl_6 \cdot 6H_2O$ and $RuCl_3 \cdot 3H_2O$.

Analytical electron microscopy of the bimetallic catalysts. It is important to note that surface compositions obtained as the result of the O_2 -CO titration experiments described above are average surface compositions. They do not indicate whether bimetallic particles are actually formed nor do they give Pt/Ru ratios for individual bimetallic particles. In order to obtain this information a particle-by-particle elemental analysis is required. Additionally, it is useful to obtain individual particle Pt/Ru elemental ratios as a function of particle size. This information is of value in the interpretation of catalytic data.

Energy dispersive X-ray spectroscopy (EDXS) data for the catalyst with an average Pt/Ru ratio of 0.5 are shown in Table 3. These data are arranged in order of increasing particle size. It is noteworthy that both Pt and Ru were present in each of the individual 24 metal particles analyzed. Monometallic particles consisting of either Ru or Pt were not found, indicating that the catalyst was composed entirely of bimetallic particles. A significant finding in this study was that the overall percentage of Pt present in the bimetallic particles increased with increasing particle size. Large particles were Pt rich and small particles were Ru rich. The Pt/Ru data shown in Table 3 is plotted as a function of particle size and is shown in Fig. 7 together with the particle size distribution. Although the large particles are strongly enriched in Pt, the number of particles having a particle size in excess of 5.0 nm is very small. Because most of the bimetallic particles are in the 1.0- to 3.0-nm range, we conclude that the catalytic properties of the catalyst are dominated by

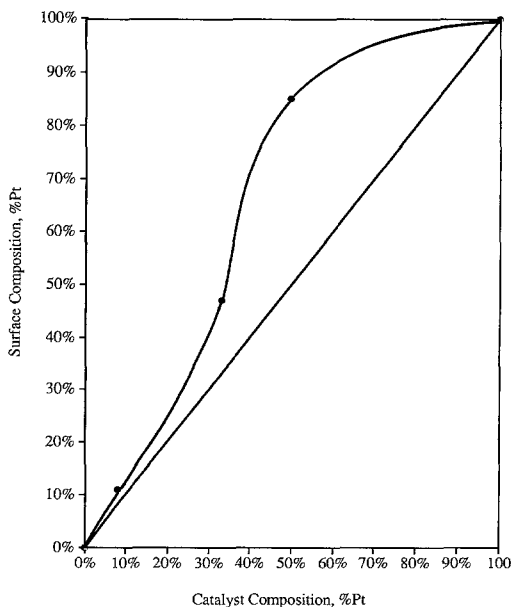


Fig. 6. Surface composition as a function of catalyst composition.

TABLE 3

EDXS Analysis of Bimetallic Pt-Ru/SiO₂
(Pt/Ru = 0.5)

	<i>D</i> (Å)	% Pt ^a	% Ru ^a	Pt/Ru
1	<10	32	68	0.47
2	10	38	62	0.62
3	10	32	68	0.47
4	10	23	77	0.31
5	10	25	75	0.33
6	12	31	69	0.45
7	15	30	70	0.42
8	15	28	72	0.39
9	15	28	72	0.39
10	15	33	67	0.49
11	15	25	75	0.33
12	15	41	59	0.68
13	15	33	67	0.49
14	15	38	62	0.62
15	15	39	61	0.64
16	20	46	54	0.86
17	20	48	52	0.93
18	20	42	58	0.73
19	20	48	52	0.91
20	25	56	44	1.29
21	25	59	41	1.42
22	35	54	46	1.16
23	40	49	51	0.97
24	45	58	42	1.38

^a Atomic percentage.

these particles. Similar trends were observed for the bimetallic particles of the catalyst which had an overall Pt/Ru ratio of unity. The analysis of 21 representative particles (Table 4) shows that only bimetallic particles were present on the catalyst. The Pt/Ru ratio for this catalyst is plotted as a function of particle size and is shown in Fig. 8 together with the particle size distribution.

The effect of catalyst pretreatment on the formation of bimetallic particles. When the bimetallic catalyst which had a Pt/Ru ratio of 0.5 was sequentially treated with oxygen at 573 K and reduced in H₂ at 673 K, a marked segregation of the metal surface phases occurred. The analysis of 15 representative particles is shown in Table 5. Particles in excess of 8.0 nm were either Ru rich or pure Ru while particles between 2.0

TABLE 4

EDXS Analysis of Bimetallic Pt-Ru/SiO₂
(Pt/Ru = 1.0)

	<i>D</i> (Å)	% Pt ^a	% Ru ^a	Pt/Ru
1	15	39	61	0.64
2	15	33	67	0.49
3	20	41	59	0.70
4	20	27	73	0.38
5	20	47	53	0.88
6	20	49	51	0.96
7	20	39	61	0.64
8	25	51	49	1.06
9	25	58	42	1.36
10	25	55	45	1.20
11	25	62	38	1.66
12	30	64	36	1.77
13	35	69	31	2.18
14	35	68	32	2.10
15	35	70	30	2.35
16	40	60	40	1.50
17	40	72	28	2.53
18	45	74	26	2.85
19	45	72	28	2.63
20	60	76	24	3.23
21	75	77	23	3.38

^a Atomic percentage.

TABLE 5

EDXS Analysis of Bimetallic Pt-Ru/SiO₂
(Pt/Ru = 0.5) (Oxygen-Treated at 573 K Prior to Reduction)

	<i>D</i> (Å)	% Pt ^a	% Ru ^a	Pt/Ru
1	20	94	6	14.40
2	20	97	3	37.50
3	25	90	10	8.62
4	25	86	14	6.00
5	30	94	6	14.40
6	30	90	18	4.93
7	80	55	45	1.20
8	80	31	61	0.51
9	85	23	77	0.31
10	85	16	84	0.18
11	85	0	88	0.00
12	100	0	100	0.00
13	100	0	100	0.00
14	100	0	100	0.00
15	100	0	100	0.00

^a Atomic percentage.

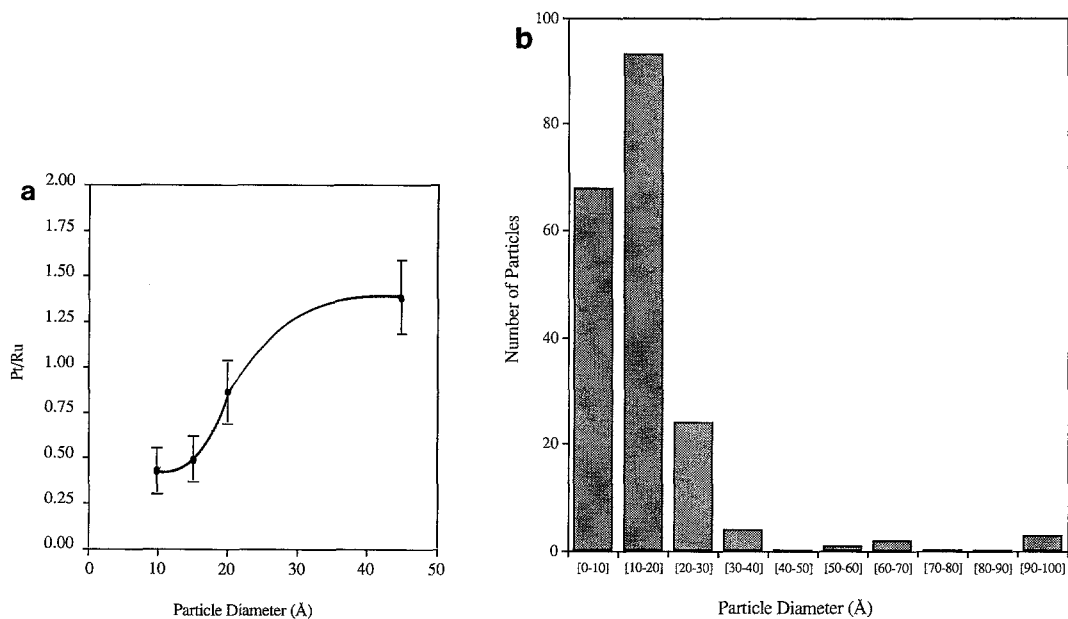


FIG. 7. (a) EDXS analysis of individual particles of Pt-Ru/SiO₂ (Pt/Ru = 0.5). (b) Particle size distribution of Pt-Ru/SiO₂ (Pt/Ru = 0.5).

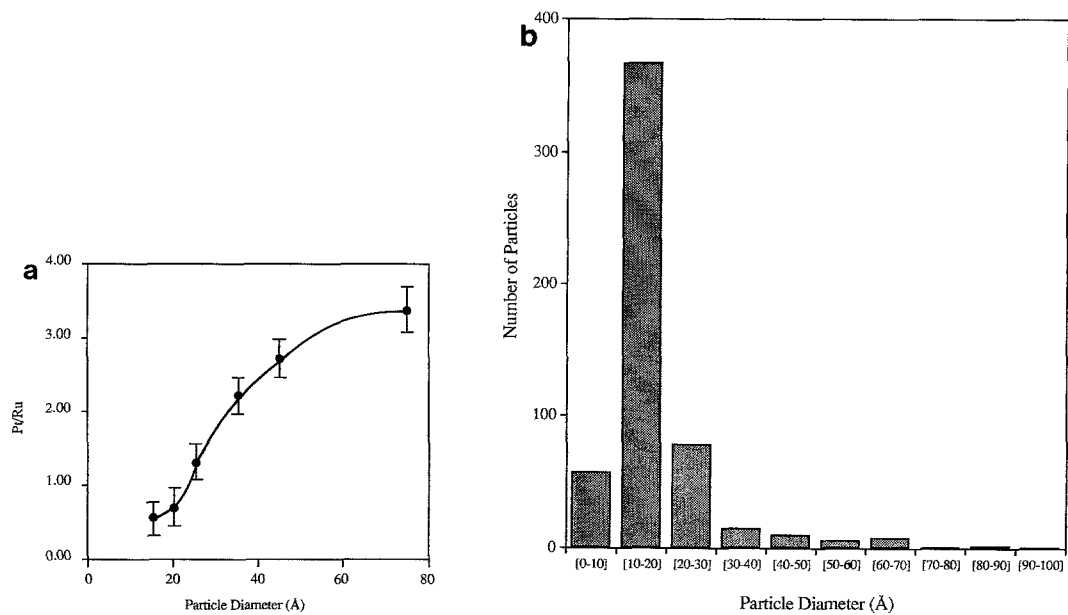


FIG. 8. (a) EDXS analysis of individual particles of Pt-Ru/SiO₂ (Pt/Ru = 1.0). (b) Particle size distribution of Pt-Ru/SiO₂ (Pt/Ru = 1.0).

and 3.0 nm were strongly enriched in Pt. Under these conditions a bimodal distribution was obtained. The large particles were either pure Ru or Ru rich as a result of the formation of RuO₂ during oxygen pretreatment.

Bimetallic catalysts prepared by sequential impregnation. Because all of the bimetallic catalysts prepared by coimpregnation showed substantial surface enrichment in Pt, it was concluded that the Pt precursor was more mobile on the surface during H₂ reduction than the Ru precursor. Identical behavior was shown to occur for bimetallic catalysts prepared by coimpregnation using H₂PtCl₆ · 6H₂O and RuCl₃ · 3H₂O. For this reason, it was decided to prepare the bimetallic catalysts by sequential impregnation. In the first step, a Pt/SiO₂ catalyst was prepared and this was then followed by sequentially impregnating this catalyst with [Ru(NH₃)₆]³⁺. The analysis of 10 representative particles for the catalyst prepared by sequential impregnation shows quite clearly that bimetallic particles were not formed (Table 6). The small particles were Ru (1–1.5 nm) while the larger particles (2.5–3.0 nm) were Pt. Apparently the Ru surface complex is not sufficiently mobile to diffuse across the support during pretreatment and nucleate atop the Pt particles.

TABLE 6

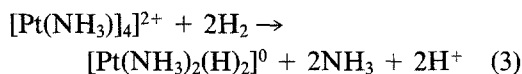
EDXS Analysis of Bimetallic Pt-Ru/SiO₂ Prepared by Sequential Impregnation

	<i>D</i> (Å)	% Pt ^a	% Ru ^a	Pt/Ru
1	10	1	99	0.01
2	10	3	97	0.03
3	12	1	99	0.01
4	12	4	96	0.04
5	15	1	99	0.01
6	15	1	99	0.01
7	25	98	2	49.00
8	30	97	3	32.33
9	30	94	6	15.67
10	30	95	5	19.00

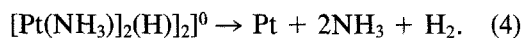
^a Atomic percentage.

DISCUSSION

The role of oxygen during pretreatment is interesting and deserves further comment. In a previous study performed by Dalla Betta and Boudart (18) [Pt(NH₃)₄]²⁺ was used as a precursor in the preparation of a zeolite-supported Pt catalyst. Higher dispersions were observed when reduction was preceded by treatment in oxygen. The explanation given by these authors suggested that a surface complex with zero charge was formed as an intermediate during reduction with H₂. The formation of this mobile precursor species can be represented as follows:

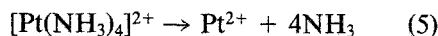


Because this precursor has zero charge, it does not interact strongly with the support and can diffuse rapidly across the support during pretreatment. This may result in the aggregation of Pt to form larger particles. Final reduction occurs according to the equation,



The final reduction step may occur as the result of a mobile Pt precursor species interacting with reduced Pt sites in the presence of chemisorbed hydrogen. For this reason, dispersions obtained by the direct reduction of [Pt(NH₃)₄]²⁺ with H₂ are not particularly high (*D* ~ 40%).

Treatment with oxygen at 573 K prior to reduction in hydrogen prevents the formation of the mobile [Pt(NH₃)₂(H)₂]⁰ intermediate. Decomposition in oxygen leads to the direct formation of Pt²⁺ by the following competing reaction:



Because no change in the charge of the surface complex occurs as a result of decomposition in oxygen, the surface mobility of the Pt species is not significant. This Pt²⁺ species is subsequently reduced in hydrogen flow resulting in a much higher dispersion (*D* ~ 80%).

Treatment of the Ru metal precursor $[\text{Ru}(\text{NH}_3)_6]^{3+}$ with oxygen prior to reduction results in the formation of large particles of RuO_2 . This effect has previously been reported by Lin *et al.* (19) and by Pearce *et al.* (17) for catalysts prepared from the same precursor on alumina and Y-zeolite, respectively. Analysis of the Ru metal content prior to and after treatment with oxygen at 573 K shows that Ru was not lost through the formation of the more volatile RuO_4 species. Ru agglomeration and crystal growth undoubtedly occurs during oxygen treatment. When oxygen was excluded and the Ru metal precursor was reduced directly in a flow of hydrogen, excellent Ru dispersions were obtained ($D \sim 70\%$). It should be noted that if this highly dispersed catalyst is treated in flowing oxygen at 673 K, the dispersion is sharply reduced to about 10%. These results show that RuO_2 can also be formed directly from metallic Ru through treatment with oxygen.

Because optimal pretreatment conditions for the two metal precursors used in this study were quite different, a decision regarding the best choice of pretreatment conditions leading to the highest possible bimetallic dispersion had to be made. Considering the possible alternatives, it was clear that direct reduction in hydrogen was the better choice.

The diffuse UV reflectance data clearly shows that both $[\text{Pt}(\text{NH}_3)_4]^{2+}$ and $[\text{Ru}(\text{NH}_3)_6]^{3+}$ are adsorbed on the surface of silica without decomposition taking place. However, the data in Table 1 show that the total metal loading of $[\text{Pt}(\text{NH}_3)_4]^{2+}$ exceeds that of $[\text{Ru}(\text{NH}_3)_6]^{3+}$ by 40%. This higher loading of the strongly adsorbed Pt surface complex can be rationalized on the basis of surface charge and steric requirements.

Peri and Hansley (20) have suggested that, for a typical oxide support, the specific concentration of surface sites, N_s , is 5×10^{18} sites/m² of support. Based on this value and the particular properties of the silica support used in this study, an upper limit for the adsorption of precursor ions on

the surface of silica can be calculated using the equation,

$$C_{\max} = \left(\frac{N_s}{N_0}\right) B_i S_{\text{ox}}, \quad (6)$$

where N_s/N_0 represents the number of moles of adsorption surface sites per square meter of support, B_i is the number of precursor ions adsorbed per surface site, and S_{ox} is the surface area per gram of support. Noting that the Pt precursor carries a charge of +2 compared to +3 for Ru, the calculated values of C_{\max} are 0.55 mmol/g support for Ru and 0.83 mmol/g support for Pt. The ratio of these maximum surface concentrations based only on charge considerations is Pt/Ru = 1.5, which is close to the value experimentally observed for the adsorption of the pure metal precursors.

Superimposed on the effect of charge, consideration must be given to steric effects. Based on the assumption that each precursor ion adsorbed on the surface is surrounded by a ring of water molecules and from a knowledge of the diameter of the precursor, the maximum number of precursor ions which can be adsorbed on the surface in a close-packed structure can be estimated (21). The maximum values for the concentration of adsorbed precursors predicted by this approach are 0.4 and 0.34 mmol metal/g of support for Pt and Ru, respectively. These values are lower than those predicted on the basis of charge considerations by a factor of about 2. Because experimental values for the adsorbed metal precursor species are well below those predicted by steric considerations, we are of the opinion that steric factors are not important and that the composition of the adsorbed precursor layer is dominated by surface charge considerations.

Because of these considerations, it is reasonable to assume that bimetallic catalysts prepared by coimpregnation are enriched in Ru. This is consistent with the fact that the Ru metal precursor carries a larger positive charge and is the more strongly bound of the two metal precursors. This observation

also explains surface enrichment in Pt. We believe that the formation of a mobile [Pt(NH₃)₂(H)₂]⁰ species during pretreatment in hydrogen results in the rapid surface diffusion of this species. Reduction atop Ru surface sites is promoted by the presence of chemisorbed hydrogen atoms.

These results are entirely consistent with the observation that bimetallic particles are not formed when the sequential impregnation of Pt/SiO₂ with [Ru(NH₃)₆]³⁺ is performed. The Ru metal complex is strongly bound to the surface. This leads to the formation of separate Pt and Ru particles as evidenced by EDXS observations.

The EDXS studies show considerable enrichment in Pt for the case of the large bimetallic particles. This observation is consistent with dispersions obtained using the pure metal precursors. Ru tends to form small metal particles (~1.0–1.5 nm) while the Pt particles are considerably larger (2.0–3.0 nm). For this reason, one would naturally expect the larger bimetallic particles to be enriched in Pt. However, because the number of large bimetallic particles is relatively small (see particle size distributions, Figs. 7b and 8b), one would expect that the catalytic properties of the resulting bimetallic catalysts to be dominated by the surface composition of the small bimetallic particles which represent a very large fraction of the total metal surface area exposed.

CONCLUSIONS

The following conclusions emerge from these studies:

(1) Highly dispersed Pt-Ru/SiO₂ bimetallic catalyst can be prepared using metal precursors which interact strongly with the support. Furthermore, this study supports previous published results in which it is proposed that bimetallic particles are formed when one of the surface phases is mobile with respect to the other.

(2) Diffuse UV reflectance studies show that the structure of the precursors is preserved upon adsorption at an appropriate solution pH.

(3) Pretreatment in oxygen at 573 K results in particle growth for Ru while suppressing the surface mobility of Pt.

(4) The Pt-Ru bimetallic particles show a significant surface enrichment in Ru.

(5) The elemental analysis of individual bimetallic particles show that small particles are Ru rich while large particles are enriched in Pt.

(6) The sequential impregnation of Pt/SiO₂ with [Ru(NH₃)₆]³⁺ result in segregated Pt and Ru particles.

(7) Pretreatment of the adsorbed phases of Ru and Pt with oxygen at 573 K results in a bimodal distribution. The large particles are pure Ru while the small particles are Pt. Bimetallic particles were not found.

ACKNOWLEDGMENTS

The authors acknowledge support from the U.S. Department of Energy (Grant DOEFG02-86ER-1351) for this research. We also acknowledge the Electron Microscopy Facility at the University of Illinois at Chicago for the use of their facility. Finally, we thank Dr. Tom Kelley and Mr. Richard Casper from the Department of Material Science at the University of Wisconsin-Madison not only for making their microscope available to us but for all of their extremely valuable assistance in performing the AEM analyses.

REFERENCES

1. Miura, H., Suzuki, T., Ushikubo, Y., Sugiyama, K., Matsuda, T., and Gonzalez, R. D., *J. Catal.* **85**, 331 (1984).
2. Miura, H., Feng, S. S., Saymeh, R., and Gonzalez, R. D., *ACS Symp. Ser.* **25**, 294 (1985).
3. Alerasool, S., Boecker, D., Rejai, B., Gonzalez, R. D., del Angel, Azomosa, M., and Gomez, R., *Langmuir* **4**, 1083 (1988).
4. Augustine, S. M., Sachtler, W. M. H., Butt, J. B., Nacheff, M. S., and Tsang, C. M., in "Proceedings, 9th International Congress on Catalysis, Calgary, 1988" (M. J. Phillips and M. Ternan, Eds.), Vol. 3, p. 1190. Chem. Institute of Canada, Ottawa, 1988.
5. Gonzalez, R. D., *Appl. Surf. Sci.* **19**, 181 (1984).
6. Hong, A. J., McHugh, B. J., Bonneimot, L., Resasco, D. E., Weber, R. S., and Haller, G. L., in "Proceedings, 9th International Congress on Catalysis, Calgary, 1988" (M. J. Phillips and M. Ternan, Eds.), Vol. 3, p. 1198. Chem. Institute of Canada, Ottawa, 1988.
7. Williams, F. L., and Nason, D., *Surf. Sci.* **45**, 377 (1984).
8. Brunelle, J. P., *Pure Appl. Chem.* **50**, 1211 (1978).

9. Subramanian, S., Noh, J. S., and Schwarz, J. A., *J. Catal.* **114**, 433 (1988).
10. Miura, H., Taguchi, H., Sugiyama, K., Matsuda, T., and Gonzalez, R. D., *J. Catal.* **124**, 194 (1990).
11. Narita, T., Miura, H., Ohira, M., Sugiyama, T., Matsuda, T., and Gonzalez, R. D., *J. Catal.* **103**, 492 (1987).
12. Narita, T., Miura, H., Ohira, M., Sugiyama, T., Matsuda, T., and Gonzalez, R. D., *J. Appl. Catal.* **32**, 185 (1987).
13. Miura, H., Hondou, N., Sugiyama, K., Matsuda, T., and Gonzalez, R. D., in "Proceedings, 9th International Congress on Catalysis, Calgary, 1988" (M. J. Phillips and M. Ternan, Eds.), Vol. 3, p. 1307. Chem. Institute of Canada, Ottawa, 1988.
14. Sarkany, J. and Gonzalez, R. D., *J. Catal.* **76**, 75 (1983).
15. Del Angel, G., Alerasool, S., Dominguez, J. M., Gomez, R., and Gonzalez, R. D., *Surf. Sci.*, in press.
16. Anderson, J. R., "Structure of Metallic Catalysts," p. 178. Academic Press, London/New York, 1975.
17. Pearce, J. R., Gustafson, B. L., and Lunsford, J. H., *Inorg. Chem.* **10**, 2957 (1981).
18. Dalla Betta, R. A. and Boudart, M., in "Proceedings, 5th International Congress on Catalysis" (J. W. Hightower, Ed.), p. 1329. North-Holland, Amsterdam, 1973.
19. Lin, Z. Z., Okuhara, T., and Misono, M., *J. Phys. Chem.* **92**, 723 (1988).
20. James, R. O. and Healy, T. W., *J. Coll. Int. Sci.* **40**, 42 (1972).
21. Regalbuto, J. R., private communication.